Cationic UV-curing of bio-based epoxidized castor oil vitrimers with electrically conductive properties

Reactive and Functional Polymers 200 (2024) 105936

Contents lists available at ScienceDirect

Reactive and Functional Polymers

journal homepage: www.elsevier.com/locate/react

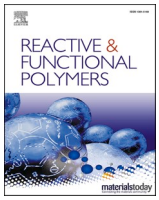

Cationic UV-curing of bio-based epoxidized castor oil vitrimers with electrically conductive properties

Matteo Bergoglio [a], Gabriele Palazzo [a], David Reisinger [b,d], Matilde Porcarello [a], Galder Kortaberria [c], Sandra Schlögl [b,d], Marco Sangermano [a,*]

[a] Politecnico di Torino, Department of Applied Science and Technology, Corso Duca degli Abruzzi 24, 10129 Torino, Italy
[b] Polymer Competence Center Leoben GmbH, Roseggerstrasse 12, 8700 Leoben, Austria
[c] Department of Chemical and Environmental Engineering, University of the Basque Country (UPV/EHU), Donostia, Spain
[d] Institute of Chemistry of Polymeric Materials, Montanuniversitaet Leoben, Otto Glöckel-Straße 2, 8700 Leoben, Austria

ARTICLE INFO

Keywords:
Bio-based epoxy monomers
Vitrimers
Cationic photopolymerization
Conductive films

ABSTRACT

The growing appeal of carbon nanotube composites in the contemporary market derives from their exceptional thermal and chemical stability, coupled with electrical conductivity. In this study, we combined these salient features with a biobased epoxy matrix having vitrimeric properties, hence being reprocessable and resheapable, to obtain a biobased conductive coating. Epoxidised castor oil (ECO) was chosen as a monomer precursor for the straightforward synthesis. The synthesis relied on a cationic UV-curing process, embedding the conductive carbon nanotubes in the matrix. Photo DSC and transmission FTIR analysis were conducted to determine the final conversion of the epoxy rings in the cationic photocuring process. Thermo-mechanical properties were evaluated by tensile tests, and DMTA. Thermal stability was assessed by TGA. Dielectric spectroscopy confirmed increased electrical conductivity in the presence of increasing CNT content, reaching a percolation threshold at 0.5 phr of CNTs. Vitrimeric properties were proved by stress relaxation experiments, and the UV-cured composite underwent a thermo-activated transesterification reaction starting from 70 °C, catalysed by dibutyl phosphate. Overall, the ECO-CNT composite showed high thermal resistance (up to 400 °C) electrical conductivity with 0.5 phr CNT concentration, and vitrimeric properties. The study can be, therefore, considered a promising starting point to obtain sustainable biobased and electrically conductive vitrimers.

1. Introduction

Vitrimers are crosslinked polymeric materials able to reorganise their topology by dynamic associative exchange reactions (Covalent Adaptable Network, CAN's). Heating vitrimers above a certain temperature leads to a gradual decrease in viscosity, and the crosslinked polymer network can be reshaped and recycled. The concept of vitrimers represents a valid compromise between the peculiar properties of thermosets and thermoplastics [1–4]. Below a certain critical temperature, the material shows the same characteristics as thermosets, such as good thermomechanical resistance and chemical inertness. However, at the same time, through a thermal stimulus, it is possible to activate the dynamic exchange reactions of the bonds, thus obtaining a decreasing trend of the viscosity as a function of the temperature, allowing recyclability and re-shapeability, like a thermoplastic material [5–11].

The concept of CANs dates back to 1956 when an original work by Tobolsky et al. [11] determined the chemical stress relaxation behaviour between 90 °C and 130 °C of polyester urethane elastomers and a polyether elastomer. In 2011, Leibler et al. [12] pioneered a cutting-edge novelty in the field of polymer chemistry: the authors redefined the chemistry of cross-linked polymers, adding specific catalysts capable of thermally activating transesterification reactions within the cross-linked structure, which led to bond exchange reactions. Therefore, a gradual reduction of the viscosity with the temperature was observed, typical of silica-based glasses, hence the name "vitrimers".

Many chemical reactions have been used to successfully achieve a bond exchange process, e.g. transesterification, transcarbamoylation, transthiocarbamoylation, imine-amine exchange, transamination of vinylogous urethanes, olefin metathesis, disulfide interchange and many others. Dynamic transesterification reactions are among the most studied processes when dealing with vitrimers, where an ester reacts with an alcohol, usually in the presence of an acid catalyst. This process has been

* Corresponding author.
E-mail address: marco.sangermano@polito.it (M. Sangermano).

https://doi.org/10.1016/j.reactfunctpolym.2024.105936
Received 4 February 2024; Received in revised form 2 May 2024; Accepted 4 May 2024
Available online 5 May 2024

observed to provide fast exchange kinetics, particularly in epoxy-based systems [5,13–17].

Implementing dynamicity in crosslinked polymeric materials can be a promising strategy to achieve sustainable and recyclable thermosets. Furthermore, the use of bio-based polymeric precursors holds great promise for the development of sustainable materials.

Recently, various thermoset resins have been obtained from natural products, such as vegetable oils, lignin, cellulose, natural carboxylic acids or natural rubber latex, which may be treated chemically to obtain the functional groups necessary to activate vitrimeric behaviour [18–23]. Therefore, integrating vitrimer properties with bio-based materials appears to be a great combination of choices.

Different review papers have been addressed by our group on the exploitation of bio-based precursors in the UV-curing process [24,25] and, in particular, integrating vitrimeric properties with biobased materials [4].

In previous works, we have investigated the sustainability of UV-curable processes by studying the reactivity of bio-based monomers towards both radical [26,27] and cationic [28,29] mechanisms. Photocured vitrimers were also studied with locally controllable photoactivation of vitrimeric properties in a covalently crosslinked thiol-epoxy network [30].

UV-cured epoxidized castor oil was investigated as vitrimeric material by exploiting transesterification bond exchange reactions at high temperatures thanks to dibutyl phosphate as a transesterification catalyst [31]. As a matter of fact, epoxidized castor oil (ECO) represents an attractive starting point as a monomer since it is possible to modify its chemical structure, tailoring it to the needs of the process: for example, ECO constitutes an inexpensive bio-renewable monomer, obtainable by an efficient and relatively cheap epoxidation process [32–35].

Within this frame, we were interested in investigating the possibility of obtaining UV-cured bio-based vitrimeric materials that add further functionalities to the crosslinked films, such as electrically conductive properties. The addition of CNTs to polymeric matrices to induce electrical conductivity is widely reported in the literature [36–43].

In this study, we dispersed CNTs into the UV-curable ECO monomer, and the formulations were photo-cured using triaryl sulfonium hexafluorophosphate salt (THS) as a photo-initiator. The transesterification reaction to activate vitrimeric properties was catalysed by the dispersion of dibutyl phosphate. The reactivity of the different formulations was investigated by means of FTIR and photo-DSC measurements. The UV-cured films were fully characterized from a thermo-mechanical point of view. When CNTs were added to the photocurable formulations, conductivity tests were performed on crosslinked materials, and finally, the vitrimeric properties were assessed by stress relaxation studies.

2. Materials and methods

2.1. Materials

Epoxidized castor oil (ECO) was purchased from specific polymers, dibutyl phosphate (DP) and triaryl sulfonium hexafluorophosphate salt (THS) were purchased from Sigma Aldrich. The carbonaceous filler used was Multi-Walled Carbon Nanotubes (CNTs) NC3100 having average dimensions of 9.5 nm × 1.5 μm, kindly provided by Nanocyl.

2.2. Formulation and photo-curing process

The ECO bio-based resin was mixed with the cationic photo-initiator at 2 phr, the transesterification catalyst and a variable amount of CNTs. To improve the components' dispersion, ECO was pre-heated at 50 °C. The four components, castor oil, photoinitiator, CNTs and transesterification catalyst, were mixed following previous studies reported in the literature [44–47]. Carbon nanotubes were previously dispersed in acetone and subsequently added to other components. The mixture was then mixed using an IKA T ULTRA-TURRAX (Staufen im Breisgau, Germany) for 90 min. During this operation, an ice bath guaranteed low temperature, to avoid thermic fluctuations. Subsequently, the system underwent further mixing in a GT sonic ultrasonic bath (Guangdong, China) at 50 °C for 2 h, to facilitate the full evaporation of acetone. After the procedure, the mixture was homogeneously mixed with the absence of aggregates. Four different formulations were prepared based on variable concentration of CNTs: pristine formulation, 0.1, 0.25, and 0.5 per hundred ratio (phr), while the cationic photoinitiator and the transesterification catalyst were kept constant at 2 and 15 phr, respectively. Once prepared, the formulations were poured into silicon molds and UV-cured using DYMAX ECE Flood lamp (Dymax Europe GmbH) at a light intensity of 130 mW/cm^2 for 60 s.

2.3. Characterization methods

2.3.1. Attenuated total reflectance Fourier transform infrared spectroscopy (ATR-FTIR)

A Nicolet iS 50 Spectrometer was used to monitor the crosslinking reaction. The liquid formulation was applied onto a silicon wafer substrate through a stir bar with a sample thickness of 32 μm. Spectra resolution was set at 4 cm^{-1}, and data processing was performed using OMNIC software from Thermo Fisher Scientific.

The conversion data was obtained by analysing the peak decreasing at 755 cm^{-1}. The peak at 2950 cm^{-1} was taken as a reference since the C—H stretching was considered unaffected by UV light. Eq. (1) was used to determine the percentage conversion.

$$Conversion\ (\%) = \frac{\left(\frac{A_{group}}{A_{ref}}\right)_{t=0} - \left(\frac{A_{group}}{A_{ref}}\right)_{t}}{\left(\frac{A_{group}}{A_{ref}}\right)_{t=0}} \times 100 \quad (1)$$

Where A_{group} is the area of the selected group under investigation, and A_{ref} is the reference area of the peak situated at 2950 cm^{-1}. The study was done during exposure time to elaborate the conversion curve.

2.3.2. Photodynamic scanning calorimetry (photo-DSC)

The crosslinking reaction was studied through photo-DSC measurement. The instrument consists of a Mettler Toledo DSC-1 (Milano, Italy) equipped with gas-controlled GC100 and a mercury Hamamatsu LIGHTINGCURE LC8 (Hamamatsu Photonics) lamp, used with an optic fibre to focalise the radiation. The UV-light wavelength is centred around 365 nm, with a 50 mW/cm^2 intensity. 5 to 15 mg of the sample was placed into an open aluminium pan, while an open pan was used as a reference. All the tests were performed under 40 ml/min nitrogen flow at room temperature (25 °C). The method consisted of two steps, each of 120 s of UV light irradiation, preceded by 60s with the lamp off. The second exposition was subtracted from the first one to eliminate the eventual noise peak not intrinsic to the material.

All the data were elaborated by Mettler Toledo STARe software V9.2.

2.3.3. Dynamic mechanical thermal analysis (DMTA)

The DMTA analysis of the UV-cured materials were conducted using a Triton Technology device in tension mode modality with a frequency of 1 Hz. The starting temperature was settled to −20 °C, with the aim of liquid nitrogen, and was stopped at 100 °C, using a heating ramp of 5 °C/min. The scope of the analysis was to determine the glass transition temperature corresponding to the maximum of the tan δ curve. The maximum temperature of the test (100 °C) was settled after the rubbery plateau of the material. The analyzed samples had a dimension of 0.5 × 7.5 × 17.5 mm, obtained by pouring liquid formulation into a silicon mould of the chosen dimension and irradiating with a DYMAX ECE Flood lamp (Dymax Europe GmbH) at a light intensity of 130 mW/cm^2 for 90 s each layer.

2.3.4. Tensile measurements

Stress-strain curves were evaluated to determine the mechanical properties of the UV-cured materials using a tensile instrument (MTS QTestTM/10 Elite, MTS System Corporation) combined with measurement software (TestWorks® 4, MTS System Corporation). The translation speed was set to 5 mm/min, and the dimensions of the samples had an average of 2 × 5 × 50 mm^3. 5 samples were tested to determine the average elastic modulus, determined in the elastic region of the curve.

2.3.5. Thermogravimetric analysis (TGA)

The thermogravimetric analysis was conducted using a Mettler Toledo TGA/DSC1 thermogravimetric analyser using 70 uL Al_2O_3 crucibles. Under a nitrogen flow of 40 ml/min, about 10 mg of sample were heated from 25 to 850 °C. The heating rate was set to 10 °C/min.

2.3.6. Electric conductivity

Broadband dielectric spectroscopy was used for measuring the electric conductivity of materials. Measurements were carried out using a Novocontrol Alpha high-resolution analyser with an applied AC voltage of 1.0 V, from which frequency-scans (isothermal spectra) were obtained. Frequency scans were measured in the range between 0.1 and 106 Hz at room temperature. Regarding sample preparation, films were hot-pressed in between two gold-plated electrodes (diameter of 20 mm) in a sandwich configuration. Initially, the thickness of the film was determined as the difference in thickness between both electrodes before and after hot-pressing the polymer film. However, the above value was corrected by measuring the thickness of the peeled-off film from the electrodes after the dielectric measurements.

2.3.7. Dynamic reversible network analysis

Stress relaxation experiments were conducted on the UV-cured sample by a Physica MCR 501 rheometer from Anton Paar (Graz, Austria). The sample dimension corresponded to 0.5 mm thickness x 1 mm diameter. The samples were first applied for 15 min at a constant temperature, then 3% constant strain was applied, and the stress was recorded over time. The temperature chosen for the test were 70 °C, 80 °C, 90 °C, 100 °C.

The relaxation modulus G(t) was normalised by the initial modulus G measured at the start of applying the strain. The relaxation time, vitrimer-characteristic properties, was determined as the time needed by the relaxation modulus to reach 1/e, with an exponential decrease, following Eq. (2):

$$G(t) = G_{t0}e^{\left(-\frac{t}{\tau}\right)} \quad (2)$$

3. Results and discussion

In this paper, we have investigated the use of the bio-based epoxy ECO in the cationic UV-Curing process in the presence of CNTs as conductive fillers to obtain UV-Cured bio-based vitrimeric coatings with conductive properties. The chemical structure of ECO is composed of long and mobile triglyceride chains (see chemical structure in Fig. 1), which provide both epoxy, ester, and hydroxyl groups. While epoxy ring could be exploited for cationic UV-induced ring opening polymerization to achieve crosslinked polymer network, the ester and hydroxyl groups, which are part of the network structure after curing can be exploited for reversible transesterification reactions to impart to the UV-cured polymer vitrimeric properties in presence of transesterification catalyst. Finally, carbon nanotubes were added from 0.1 to 0.5 phr, to achieve electrically conductive properties of the crosslinked films (Scheme Fig. 1).

3.1. Photo-curing process

The UV-curing process of the epoxy bio-based formulations was deeply investigated through two different methods, FTIR and photo-DSC analyses. The effect of the carbon nanotubes was considered (from 0.1 to 0.5 phr), and the monomer conversion rate of the epoxy monomer was studied.

The photoinduced ring-opening photopolymerization reaction was monitored following the decreasing of the epoxy peak, centred at 775 cm^{-1}. An example of a typical FTIR spectra recorded for the pristine ECO photocurable formulation is reported in Fig. 2. The epoxy peak area decreased during the UV irradiation time, confirming both the epoxy ring opening and the consequent crosslinking reaction.

Following the Eq. (1), the conversion percentage was calculated. The conversion curves as a function of irradiation time are reported in Fig. 3.

The pristine resin achieves an almost full conversion (95% of epoxy group conversion after 120 s of irradiation). When CNTs were added to the epoxy-based resin, a slight decrease photopolymerization rate (with a decrease of the slope of the conversion versus time of irradiation curves) and of epoxy group conversion is evident by increasing the CNTs content. The formulation containing 0.1 phr of CNTs showed an almost similar conversion, while the formulation containing 0.5 phr of CNTs showed a final epoxy group conversion of about 88%, after 120 s of irradiation. This is attributed to the competitive UV adsorption by CNTs with respect to the cationic photoinitiator. In fact, CNTs absorb across a broad spectrum of UV radiation, a behaviour attributed to the resonance plasmons present in the free electron clouds of the π electrons of the CNTs [48,49]. Despite the UV light adsorption, also the formulations containing the higher content of CNTs reach a satisfactory conversion above 80%, as mentioned above.

The photo-DSC analyses were in agreement with the results obtained by the FTIR data, revealing a reduction of the exothermic peak for the formulations containing CNTs. The exothermic curves as a function of irradiation time are reported in Fig. 4. The integral of the curves is collected in Table 1 together with the peak, the time to reach the peak of

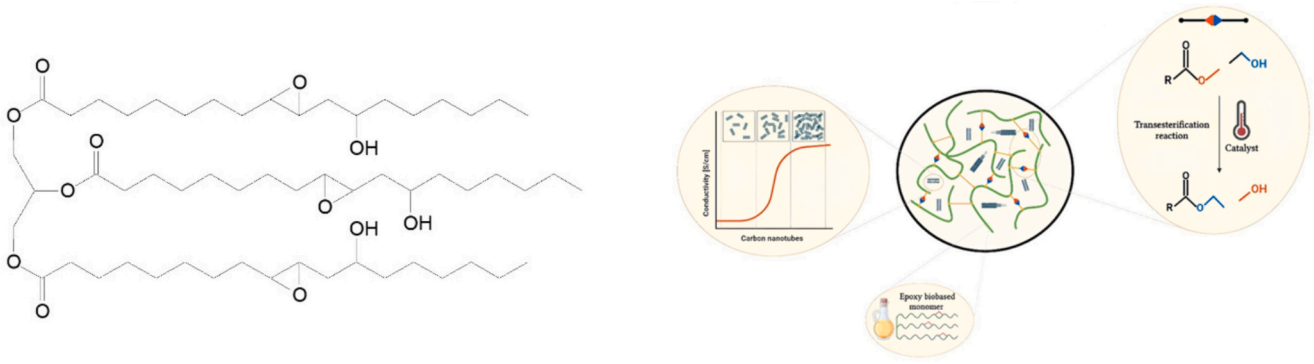

Fig. 1. Chemical structure of epoxidized castor oil (left) and overall properties scheme (right).

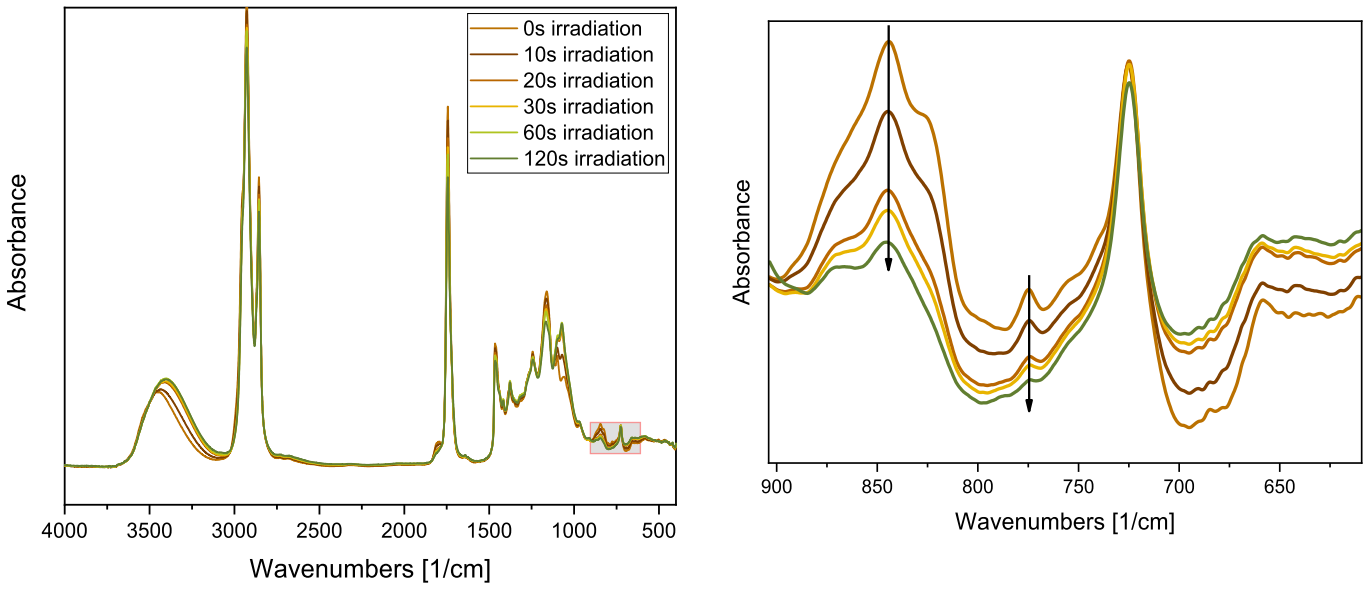

Fig. 2. Typical FTIR spectra for ECO formulations with different contents of CNTs filler as a function of UV-light irradiation. Light intensity was set to 130 mW/cm^2.

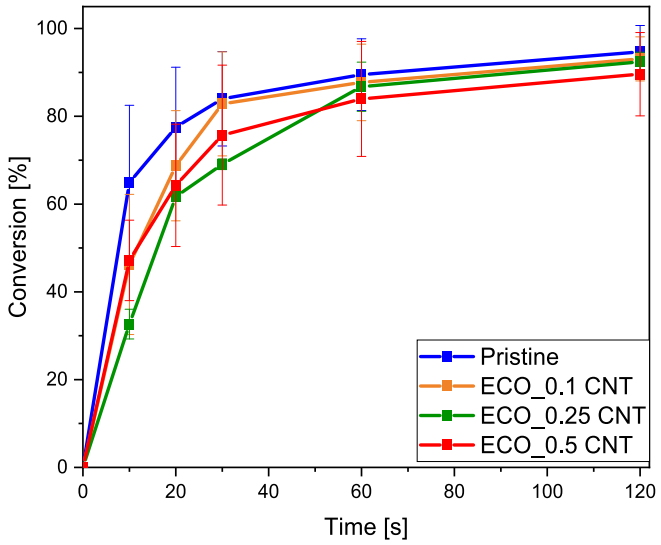

Fig. 3. Epoxy group conversion (obtained by ATR-FTIR) for ECO formulation with different contents of CNTs filler. Light intensity was set to 130 mW/cm^2.

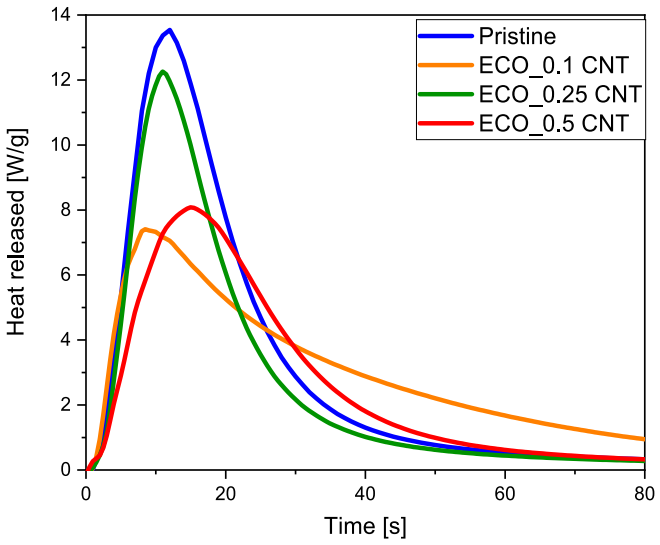

Fig. 4. Heat released during irradiation of the ECO-CNTs formulations with UV-light as a function of time.

exothermicity. An almost linear decrease of the exothermicity, with a decrease of the integrated area value, is evident by increasing the CNTs content in the photocurable formulation. Formulations with the minimum amount of CNTs (0.1 phr) exhibit an exothermic peak very similar to the pristine ECO, recording a value of 229 J/g for the pristine formulation and a value of 228 J/g for the formulation containing 0.1 phr of CNTs. By increasing the CNT content to 0.5 phr the exothermicity value decreased to about 199 J/g. Furthermore, it is possible to observe an increase of t_{peak} that can be attributed to the UV-light absorbing of the CNTs filler, resulting in a deceleration of the kinetics process, as previously evidenced by FTIR conversion curves.

3.2. Viscoelastic, thermal and mechanical properties of cured composite

3.2.1. DMTA

Viscoelastic properties of the UV-cured formulations were tested by DMTA analysis. In Fig. 5, the tanδ curves are reported for all the investigated formulations containing different amounts of CNTs. The T_g data, taken as the maximum of tanδ peak, are collected in Table 2. The modulus value was measured at 50 °C above the T_g (modulus measured from the storage modulus curves E' not reported in the Figure).

It is possible to observe a slight decrease in the T_g values for the crosslinked materials obtained in the presence of CNTs, while the composites materials showed a were very similar T_g for all the cured samples containing increasing CNT content. Actually, the DMTA analysis showed a decrease of the T_g for the UV-cured films from 29 °C of the pristine material to 18 °C for the epoxy-based films obtained in the

Table 1
Heat released values obtained from the photoDSC analysis.

Sample	Integral (J/g)	Time to peak (s)
Pristine	229.9 ± 12.0	11.6 ± 0.6
ECO_0.1CNT	228.4 ± 4.7	10.4 ± 1.2
ECO_0.25CNT	226.5 ± 18.9	12.8 ± 1.2
ECO_0.5CNT	199.9 ± 17.2	15.0 ± 0.0

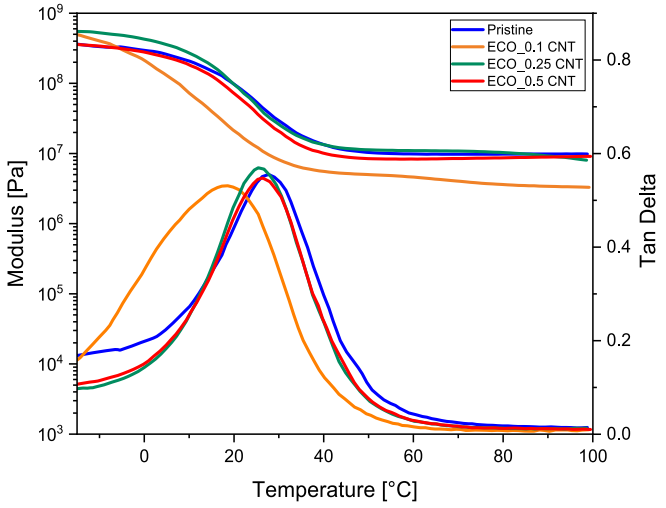

Fig. 5. Tan δ curves and relative storage modulus E' obtained from DMTA for the ECO-CNTs formulations.

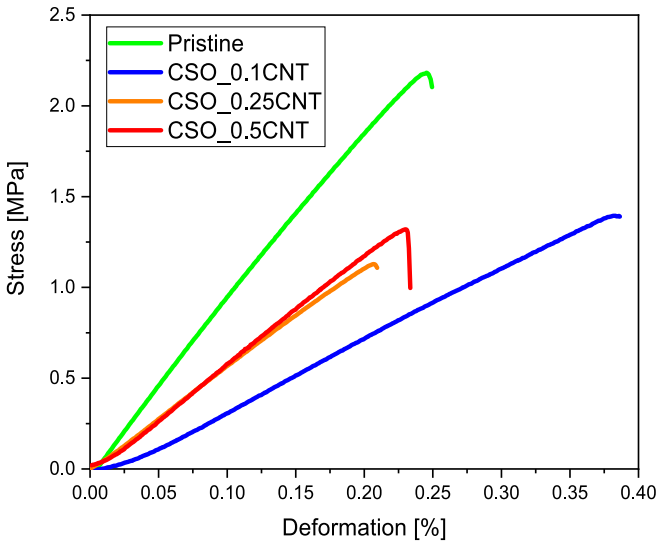

Fig. 6. Stress-strain curves obtained by tensile tests of ECO-CNT samples.

Table 2
Glass transition temperature and modulus obtained from DMTA analysis.

Sample	T_g [°C][1]	Modulus [MPa][2] measured at T_g + 50 °C
Pristine	29 ± 1	7.8 ± 2.3
ECO_0.1CNT	18 ± 2	3.0 ± 1.7
ECO_0.25CNT	24 ± 1	8.4 ± 2.1
ECO_0.5CNT	26 ± 1	8.4 ± 0.3

[1] Measured as the maximum of tanδ curves.
[2] measured in the rubbery plateaux of the E' curves.

Table 3
Elastic modulus, tensile strength, and elongation at break values obtained from tensile tests.

	Pristine	ECO_0.1CNT	ECO_0.25CNT	ECO_0.5CNT
Elastic modulus [MPa]	7.72 ± 1.87	3.59 ± 0.95	5.43 ± 1.38	5.59 ± 0.34
Tensile strength [MPa]	1.62 ± 0.60	0.90 ± 0.28	0.96 ± 0.26	1.06 ± 0.18
Elongation at break [%]	23.15 ± 3.27	27.98 ± 6.54	19.63 ± 1.46	20.99 ± 1.92

presence of 0.1 phr of CNTs. By further increasing the CNT content in the photocured material, it was possible to observe an enhancement of the T_g up to 24 °C and 26 °C, respectively, for the sample containing 0.25 phr of CNTs and 0.5 phr of CNTs. The slight flexibilization effect could be explained by the decrease of epoxy group conversion in the presence of the filler, as explained in the previous section. When CNTs content is increased, a dual effect is evident. Even if a slight decrease of epoxy group conversion would induce a decrease of crosslinking density of the polymeric network, with an expected flexibilization, when CNTs content is above 0.1 phr, it is evident that their reinforcing effect counterbalanced the flexibilization. In fact, the CNTs can hinder the mobility of the polymeric chain with an enhancement of thermo-mechanical properties, evidenced by the increase of the T_g and the modulus in the rubbery region by further increasing the CNTs content.

3.2.2. Tensile tests

Mechanical properties of UV-cured pristine epoxy resin and the crosslinked epoxy-based formulations containing CNTs were evaluated by means of a tensile test. The tensile curves are reported in Fig. 6. The Young's modulus value (E), tensile strength (σ_{ts}), and percentage elongation at break data are collected in Table 3.

A brittle behaviour is evident for all the samples, as the specimen breaks after the elastic portion of the curve. From the data reported in Table 3, it is possible to observe that adding 0.1 phr CNTs reduced mechanical performance and decreased rigidity and tensile strength but increased elongation at break. This is an additional confirmation of the effect of adding carbon nanotubes in the photocurable formulation, which reduces the overall epoxy group conversion with a reduction of crosslinking density and, therefore, a resulting flexibilization. On the other hand, a further CNTs addition leads to a gradual increase in Young's modulus and tensile strength, highlighting the dual effect of CNTs on the composite. As previously discussed, at low concentrations, the effect of reduction in epoxy group conversion is noticeable, while at higher concentrations, the reinforcing effect given by the CNTs becomes predominant. When focusing on higher concentrations (0.25 and 0.5 phr), the material becomes more brittle, as evidenced by the reduced elongation at break.

3.2.3. TGA analysis

The thermal stability of the cured formulation was studied through TGA, the typical curves for the Uv-Cured film containing 0.1 phr CNTs is reported, as an example in Fig. 7. The sample contains two main

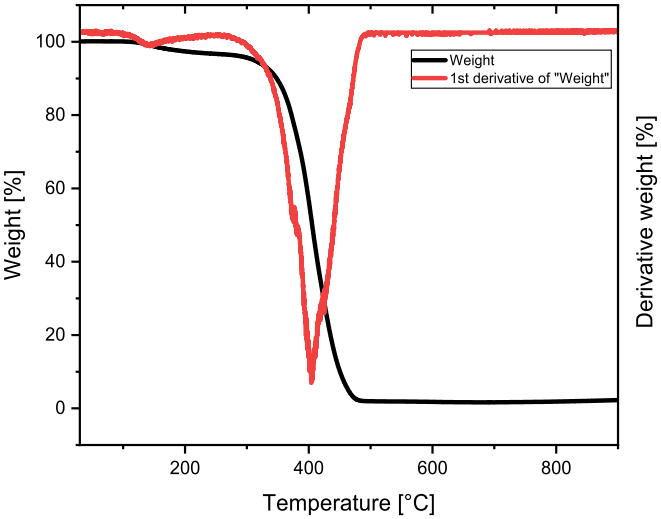

Fig. 7. Thermal degradation curve obtained by TGA for the ECO network having 0.1 phr concentration of CNTs.

degradation steps. The first degradation step is attributed to the degradation of the unreacted photoinitiator and monomers, while the step at a higher temperature, around 400 °C, regards the degradation of the cured ECO network. The carbon nanotubes are not degrading during the analysis since their thermal resistance is elevated also at high temperatures [50,51].

Similar results were achieved for the other UV-cured formulations. These results are important to define the maximum temperature accessible for the films and to investigate the activation of the transesterification reaction (see paragraph 3.4 below).

3.3. Electric conductivity

The cured films containing CNTs were characterized by means of dielectric spectroscopy to measure conductivity values for the evaluation of the percolation threshold. In Fig. 8, the conductivity values are reported as a function of the CNT content in the photocured films. It can be observed that the electrical conductivity increased for all the composites, but a sharp increase of about 7 orders of magnitude is detected for samples containing 0.5 phr of CNT. While the pristine ECO UV-cured films showed a conductivity of about 1.0 e^{-13} S/cm, the UV-cured formulation obtained in the presence of 0.5 phr of CNTs showed conductivity values of around 1.0 e^{-6} S/cm, seeming to be above the percolation threshold, behaving like a conductor. So, it can be said that the percolation threshold is between 0.25 and 0.5 phr of CNT, in agreement with that found by other authors for composites based on biobased epoxy and CNTs, in which samples with 0.4 of CNTs are already percolated [52].

3.4. Stress relaxation analysis

Stress relaxation analyses were performed on UV-cured pristine and filled epoxy-based materials to investigate the thermal activation of the dynamic transesterification, i.e. the vitrimeric properties, at elevated temperatures. In our previous work [31], we reported that the pristine UV-cured epoxidized castor oil showed vitrimeric behaviour above 100 °C. The stress relaxation of UV-cured ECO samples containing dibutyl phosphate as transesterification catalysts, recorded at different temperatures, showed that all the UV-cured formulations reached 1/e relaxation modulus at high temperatures. The relaxation time (τ) is a crucial indicator of the vitrimeric properties, which is the time needed for the sample's relaxation modulus G(t) to reach 37% (1/e) of the initial modulus detected [4,31,53]. The vitrimeric properties of UV-cured ECO were attributed to the chemical structure of the bio-based epoxy, which is composed of long triglyceride chains containing both epoxy groups exploited for UV-Curing process and esters and hydroxyl groups, fundamental for the transesterification reaction. At sufficiently high temperatures, dibutyl phosphate (DP) can catalyze the exchange reaction that occurs between ester and hydroxyl groups, which induces a change in viscosity measured by the stress relaxation experiments.

The stress relaxation measurements were performed in a temperature range from 70 to 100 °C on UV-cured samples containing 0.5 phr of CNTs, as an example. This temperature range is far away from the degradation temperature of the crosslinked composites.

The control for the test was chosen as the UV-cured epoxy-based material containing 0.5 phr of CNTs in the absence of the transesterification catalyst, compared with the same UV-cured formulation obtained in the presence of the DP catalyst. The relaxation curves recorded at 70 °C are reported in Fig. 9. As previously observed for the pristine ECO UV-cured sample [31], a slight relaxation can be also observed in the reference UV-cured materials. This could be probably due to the presence of residual photogenerated acid from the cationic photoinitiator, which can activate the transesterification reaction to a certain degree, but not enough to activate vitrimeric properties.

On the other hand, when DP transesterification catalyst is dispersed in the photocured composite materials, a decrease in the relaxation modulus is evident, reaching the value 1/e, which is reached quicker by increasing temperature. The highest temperature tested was 100 °C. The decrease in relaxation time by increasing temperature suggests an increase in transesterification rate, hence a faster rearranging of the crosslinked structure, as visible in Fig. 10.

The dynamic nature of vitrimers, governed by thermally triggered exchange reactions that facilitate network topology adjustments, follows the Arrhenius law at high temperatures. [54] Fig. 11 illustrate a linear relationship between relaxation time and temperature, providing evidence of vitrimeric properties in ECO UV-Cured films containing CNTs. The observed linear behaviour is supported by a good linear fit. Furthermore, the activation energy derived from the Arrhenius plot correspond to 49.9 kJ/mol, aligned to a typical activation energy of vitrimers. [54,55]

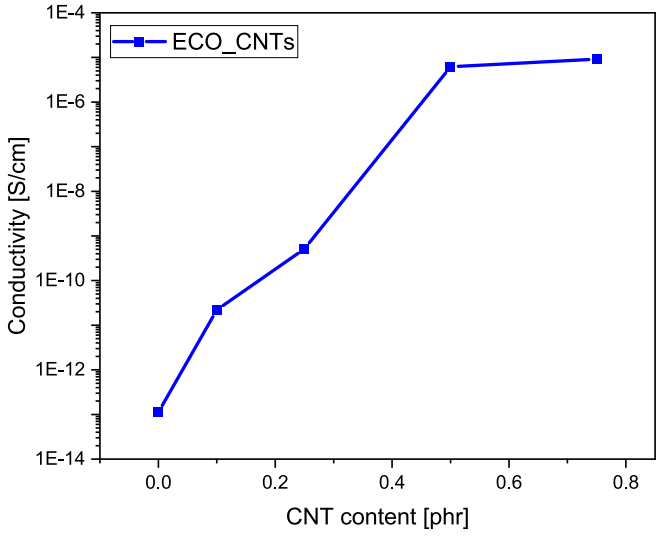

Fig. 8. Conductivity values obtained from dielectric spectroscopy test performed on UV-Cured ECO-based formulations containing increasing percentage content of CNTs.

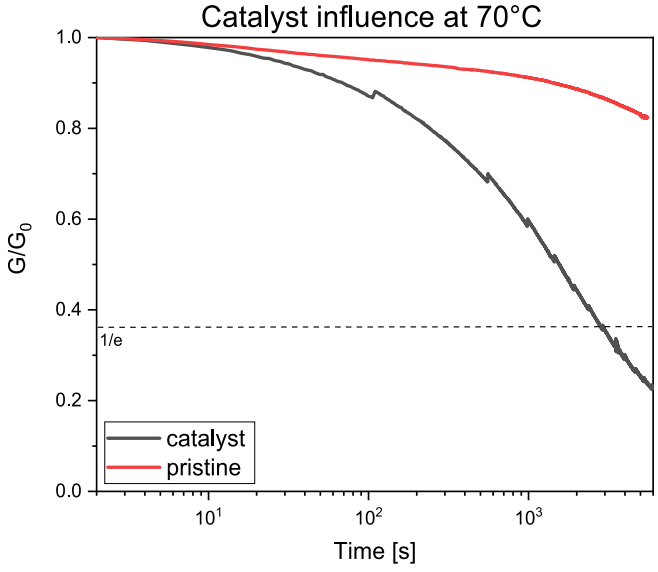

Fig. 9. Stress relaxation experiment for ECO samples containing 0.5 phr CNTs with and without transesterification catalyst at 70 °C.

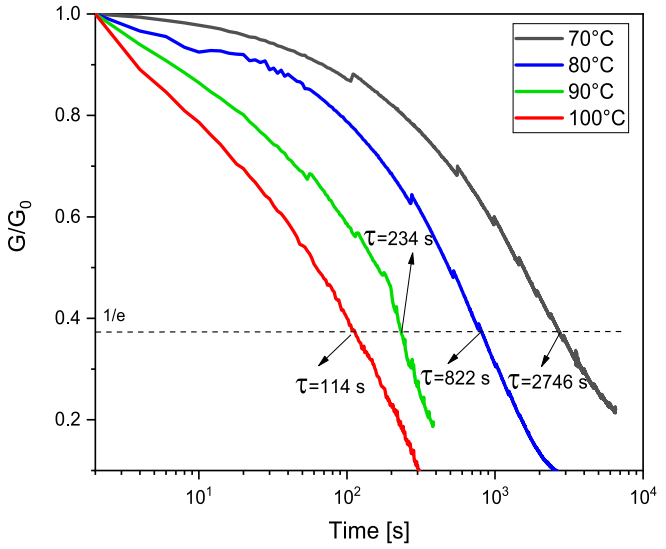

Fig. 10. Stress relaxation experiment of ECO UV-Cured composites containing 0.5 phr CNTs and transesterification catalyst. The test has been performed at different temperatures in the range between 70 °C and 100 °C.

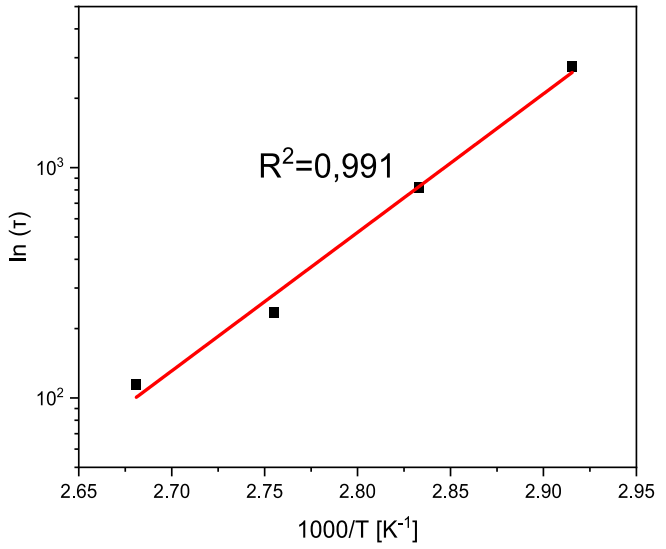

Fig. 11. Arrhenius plot of ECO composites containing 0.5 phr CNT obtained from relaxation times.

4. Conclusions

A bio-based epoxy resin was used with both dibutyl phosphate and CNTs to design a new electrically conductive vitrimeric composite. ECO reactivity towards UV-curing was investigated by means of FTIR and photo-DSC analyses. The curing tests proved the high reactivity of the pristine monomer but revealed that increasing CNT content in the photocurable formulations progressively slightly reduced the epoxy group conversion due to a competitive UV-adsorption effect of CNTs towards the cationic photoinitiator. The photo-DSC analyses confirmed the decrease of epoxy group conversion and photocuring rate by increasing the CNTs content in the photocurable formulations, evidenced both by a decrease of the total measured exothermicity of polymerization as well as by the increase of the t_{peak}.

The UV-cured pristine and filled films were characterized by DMTA, tensile tests and TGA analysis, investigating the impact of the presence of CNTs on thermal and mechanical properties of UV-Cured samples. The DMTA analysis showed a decrease of the T_g for the UV-cured films from 29 °C of the pristine material to 18 °C for the epoxy-based films containing 0.1 phr of CNTs. By further increasing the CNT content in the photocured material, it was possible to observe an enhancement of the T_g up to 26 °C for the sample with 0.5 phr of CNTs. Similarly, the tensile measurements showed an initial decrease of the mechanical properties by adding 0.1 phr of CNTs, followed by an increase of the Young's modulus and tensile strength by increasing the filler concentration. This behaviour was attributed to two different effects induced by the addition of CNTs. From one side, the presence of the CNTs competitive absorbing UV-light induced a decrease of the epoxy group conversion with a decrease of crosslinking density and, therefore, induced a flexibilization of the polymeric network. On the other side, the fillers can hinder the polymeric chain mobility inducing a reinforcement effect and enhancing the thermo-mechanical properties. This was evidenced by an increase of T_g by further increase in CNTs content as well as an increase of the modulus.

Dielectric spectroscopy was used to evaluate the conductivity of crosslinked films containing CNTs. A percolation threshold was reached at 0.5 phr CNTs' content, reaching a conductivity value of 1.0 e^{-6}, typical of a conductor. Stress relaxation experiments showed that the crosslinked material obtained in the presence of 0.5 phr CNTs reached 1/e relaxation modulus at temperatures in the range from 70 °C to 100 °C. A decrease in relaxation time was obtained with increasing temperature, suggesting an increase in transesterification rate.

In conclusion, in this study, we have demonstrated the possibility of achieving sustainable UV-cured epoxy films containing CNTs showing electrical conductivity and vitrimeric behaviour by combining bio-based precursors with environmentally friendly UV-curing techniques.

Author statement

We confirm that the manuscript has been read and approved by all named authors and that there are no other persons who satisfied the criteria for authorship but are not listed. We further confirm that the order of authors listed in the manuscript has been approved by all of us.

CRediT authorship contribution statement

Matteo Bergoglio: Investigation, Formal analysis. **Gabriele Palazzo:** Formal analysis. **David Reisinger:** Investigation. **Matilde Porcarello:** Formal analysis. **Galder Kortaberria:** Investigation. **Sandra Schlögl:** Conceptualization. **Marco Sangermano:** Supervision, Data curation, Conceptualization.

Declaration of competing interest

The authors declare that they have no known competing financial interests or personal relationships that could have appeared to influence the work reported in this article.

Data availability

No data was used for the research described in the article.

Acknowledgements

This paper is part of a project that has received funding from the European Union's Horizon 2020 research and innovation program under the Marie Skłodowska-Curie grant agreement, No 101085759 (SURE-Poly) and Ministerio de Ciencia, Innovacion y Universidades, grant number PID2021-126417NB-I00.

Stress relaxation studies of the samples were carried out within the COMET-Module project “Repairtecture” (project-498 no.: 904927) at the Polymer Competence Center Leoben GmbH (PCCL, Austria) within the framework of the COMET-program of the Federal Ministry for

Climate Action, Environment, Energy, Mobility, Innovation and Technology and the Federal Ministry of Labour and Economy. The PCCL is funded by the Austrian Government and the State Governments of Styria, Upper and Lower Austria.

References

[1] A. Kumar, L.A. Connal, Biobased transesterification Vitrimers, Macromol. Rapid Commun. (2023) 44, https://doi.org/10.1002/marc.202200892.

[2] N.J. Van Zee, R. Nicolaÿ, Vitrimers: permanently crosslinked polymers with dynamic network topology, Prog. Polym. Sci. 104 (2020) 101233, https://doi.org/10.1016/j.progpolymsci.2020.101233.

[3] W. Alabiso, S. Schlögl, The impact of Vitrimers on the industry of the future: chemistry, properties and sustainable forward-looking applications, Polymers (Basel) 12 (2020) 1660, https://doi.org/10.3390/polym12081660.

[4] M. Sangermano, M. Bergoglio, S. Schögl, Biobased Vitrimeric epoxy networks, Macromol. Mater. Eng. (2023), https://doi.org/10.1002/mame.202300371.

[5] W. Denissen, J.M. Winne, F.E. Du Prez, Vitrimers: permanent organic networks with glass-like fluidity, Chem. Sci. 7 (2016) 30–38, https://doi.org/10.1039/C5SC02223A.

[6] B. Krishnakumar, R.V.S.P. Sanka, W.H. Binder, V. Parthasarthy, S. Rana, N. Karak, Vitrimers: associative dynamic covalent adaptive networks in thermoset polymers, Chem. Eng. J. 385 (2020) 123820, https://doi.org/10.1016/j.cej.2019.123820.

[7] J.M. Winne, L. Leibler, F.E. Du Prez, Dynamic covalent chemistry in polymer networks: a mechanistic perspective, Polym. Chem. 10 (2019) 6091–6108, https://doi.org/10.1039/C9PY01260E.

[8] P. Chakma, C.N. Morley, J.L. Sparks, D. Konkolewicz, Exploring how Vitrimer-like properties can be achieved from dissociative exchange in Anilinium salts, Macromolecules 53 (2020) 1233–1244, https://doi.org/10.1021/acs.macromol.0c00120.

[9] P. Chakma, C.N. Morley, J.L. Sparks, D. Konkolewicz, Exploring how Vitrimer-like properties can be achieved from dissociative exchange in Anilinium salts, Macromolecules 53 (2020) 1233–1244, https://doi.org/10.1021/acs.macromol.0c00120.

[10] B.R. Elling, W.R. Dichtel, Reprocessable cross-linked polymer networks: are associative exchange mechanisms desirable? ACS Cent. Sci. 6 (2020) 1488–1496, https://doi.org/10.1021/acscentsci.0c00567.

[11] M. Hayashi, Implantation of recyclability and Healability into cross-linked commercial polymers by applying the Vitrimer concept, Polymers (Basel) 12 (2020) 1322, https://doi.org/10.3390/polym12061322.

[12] D. Montarnal, M. Capelot, F. Tournilhac, L. Leibler, Silica-like malleable materials from permanent organic networks, Science 2011 (334) (1979) 965–968, https://doi.org/10.1126/science.1212648.

[13] D.J. Fortman, J.P. Brutman, G.X. De Hoe, R.L. Snyder, W.R. Dichtel, M.A. Hillmyer, Approaches to sustainable and continually recyclable cross-linked polymers, ACS Sustain. Chem. Eng. 6 (2018) 11145–11159, https://doi.org/10.1021/acssuschemeng.8b02355.

[14] W. Zou, J. Dong, Y. Luo, Q. Zhao, T. Xie, Dynamic covalent polymer networks: from old chemistry to modern day innovations, Adv. Mater. 29 (2017), https://doi.org/10.1002/adma.201606100.

[15] N.J. Van Zee, R. Nicolaÿ, Vitrimers: permanently crosslinked polymers with dynamic network topology, Prog. Polym. Sci. 104 (2020) 101233, https://doi.org/10.1016/j.progpolymsci.2020.101233.

[16] Y. Jin, Z. Lei, P. Taynton, S. Huang, W. Zhang, Malleable and recyclable thermosets: the next generation of plastics, Matter 1 (2019) 1456–1493, https://doi.org/10.1016/j.matt.2019.09.004.

[17] G.M. Scheutz, J.J. Lessard, M.B. Sims, B.S. Sumerlin, Adaptable crosslinks in polymeric materials: resolving the intersection of thermoplastics and thermosets, J. Am. Chem. Soc. 141 (2019) 16181–16196, https://doi.org/10.1021/jacs.9b07922.

[18] A. Kumar, L.A. Connal, Biobased transesterification Vitrimers, Macromol. Rapid Commun. (2023) 44, https://doi.org/10.1002/marc.202200892.

[19] Y. Hu, S. Tong, Y. Sha, J. Yu, L. Hu, Q. Huang, P. Jia, Y. Zhou, Cardanol-based epoxy Vitrimer/carbon Fiber composites with integrated mechanical, self-healing, Reprocessable, and welding properties and degradability, Chem. Eng. J. 471 (2023) 144633, https://doi.org/10.1016/j.cej.2023.144633.

[20] S. Nicolas, T. Richard, J. Dourdan, L. Lemiègre, J. Audic, Shape memory epoxy Vitrimers based on waste frying sunflower oil, J. Appl. Polym. Sci. 138 (2021), https://doi.org/10.1002/app.50904.

[21] M.A. Rashid, M.N. Hasan, M.A. Kafi, Synthesis of novel vanillin-amine hardeners fully derived from renewable bio feedstocks and their curing with epoxy resins to produce recyclable Reprocessable Vitrimers, Heliyon 9 (2023) e16062, https://doi.org/10.1016/j.heliyon.2023.e16062.

[22] Y. Hu, S. Tong, Y. Sha, J. Yu, L. Hu, Q. Huang, P. Jia, Y. Zhou, Cardanol-based epoxy Vitrimer/carbon Fiber composites with integrated mechanical, self-healing, Reprocessable, and welding properties and degradability, Chem. Eng. J. 471 (2023) 144633, https://doi.org/10.1016/j.cej.2023.144633.

[23] Y. Zhang, F. Ma, L. Shi, B. Lyu, J. Ma, Recyclable, repairable and malleable bio-based epoxy Vitrimers: overview and future prospects, Curr. Opin. Green Sustain. Chem. 39 (2023) 100726, https://doi.org/10.1016/j.cogsc.2022.100726.

[24] L. Pezzana, E. Malmström, M. Johansson, M. Sangermano, UV-curable bio-based polymers derived from industrial pulp and paper processes, Polymers (Basel) 13 (2021) 1530, https://doi.org/10.3390/polym13091530.

[25] L. Pezzana, G. Melilli, M. Sangermano, N. Sbirrazzuoli, N. Guigo, Sustainable approach for coating production: room temperature curing of Diglycidyl Furfuryl amine and Itaconic acid with UV-induced thiol-Ene surface post-functionalization, React. Funct. Polym. 182 (2023) 105486, https://doi.org/10.1016/j.reactfunctpolym.2022.105486.

[26] L. Pezzana, M. Sangermano, Fully biobased UV-cured thiol-Ene coatings, Prog. Org. Coat. 157 (2021) 106295, https://doi.org/10.1016/j.porgcoat.2021.106295.

[27] L. Pezzana, G. Melilli, P. Delliere, D. Moraru, N. Guigo, N. Sbirrazzuoli, M. Sangermano, Thiol-Ene biobased networks: furan allyl derivatives for green coating applications, Prog. Org. Coat. 173 (2022) 107203, https://doi.org/10.1016/j.porgcoat.2022.107203.

[28] L. Pezzana, G. Melilli, N. Guigo, N. Sbirrazzuoli, M. Sangermano, Cross-linking of biobased Monofunctional furan epoxy monomer by two steps process, UV irradiation and thermal treatment, Macromol. Chem. Phys. 224 (2023), https://doi.org/10.1002/macp.202200012.

[29] L. Pezzana, G. Melilli, N. Guigo, N. Sbirrazzuoli, M. Sangermano, Cationic UV curing of bioderived epoxy furan-based coatings: tailoring the final properties by in situ formation of hybrid network and addition of Monofunctional monomer, ACS Sustain. Chem. Eng. 9 (2021) 17403–17412, https://doi.org/10.1021/acssuschemeng.1c06939.

[30] D. Reisinger, K. Dietliker, M. Sangermano, S. Schlögl, Streamlined concept towards spatially resolved Photoactivation of dynamic transesterification in Vitrimeric polymers by applying thermally stable Photolatent bases, Polym. Chem. 13 (2022) 1169–1176, https://doi.org/10.1039/D1PY01722E.

[31] M. Bergoglio, D. Reisinger, S. Schlögl, T. Griesser, M. Sangermano, Sustainable bio-based UV-cured epoxy Vitrimer from Castor oil, Polymers (Basel) 15 (2023) 1024, https://doi.org/10.3390/polym15041024.

[32] A. Kumar, L.A. Connal, Biobased transesterification Vitrimers, Macromol. Rapid Commun. 44 (2023) 2200892, https://doi.org/10.1002/marc.202200892.

[33] T. Vidil, A. Llevot, Fully biobased Vitrimers: future direction toward sustainable cross-linked polymers, Macromol. Chem. Phys. 223 (2022), https://doi.org/10.1002/macp.202100494.

[34] M.A. Lucherelli, A. Duval, L. Avérous, Biobased Vitrimers: towards sustainable and adaptable performing polymer materials, Prog. Polym. Sci. 127 (2022) 101515, https://doi.org/10.1016/j.progpolymsci.2022.101515.

[35] S. Chakrapani, J.V. Crivello, Synthesis and Photoinitiated cationic polymerization of Epoxidized Castor oil and its derivatives, J. Macromol. Sci. A 35 (1998) 1–20, https://doi.org/10.1080/10601329808001959.

[36] D. Nuzhnyy, M. Savinov, V. Bovtun, M. Kempa, J. Petzelt, B. Mayoral, T. McNally, Broad-band conductivity and dielectric spectroscopy of composites of multiwalled carbon nanotubes and poly(ethylene terephthalate) around their low percolation threshold, Nanotechnology 24 (2013) 055707, https://doi.org/10.1088/0957-4484/24/5/055707.

[37] E. Logakis, Ch. Pandis, P. Pissis, J. Pionteck, P. Pötschke, Highly conducting poly (methyl methacrylate)/carbon nanotubes composites: investigation on their thermal, dynamic-mechanical, electrical and dielectric properties, Compos. Sci. Technol. 71 (2011) 854–862, https://doi.org/10.1016/j.compscitech.2011.01.029.

[38] E. Logakis, Ch. Pandis, V. Peoglos, P. Pissis, J. Pionteck, P. Pötschke, M. Mičušík, M. Omastová, Electrical/dielectric properties and conduction mechanism in melt processed polyamide/multi-walled carbon nanotubes composites, Polymer (Guildf.) 50 (2009) 5103–5111, https://doi.org/10.1016/j.polymer.2009.08.038.

[39] C.-R. Yu, D.-M. Wu, Y. Liu, H. Qiao, Z.-Z. Yu, A. Dasari, X.-S. Du, Y.-W. Mai, Electrical and dielectric properties of polypropylene nanocomposites based on carbon nanotubes and barium Titanate nanoparticles, Compos. Sci. Technol. 71 (2011) 1706–1712, https://doi.org/10.1016/j.compscitech.2011.07.022.

[40] W. Shen, L. Feng, X. Liu, H. Luo, Z. Liu, P. Tong, W. Zhang, Multiwall carbon nanotubes-reinforced epoxy hybrid coatings with high electrical conductivity and corrosion resistance prepared via electrostatic spraying, Prog. Org. Coat. 90 (2016) 139–146, https://doi.org/10.1016/j.porgcoat.2015.10.006.

[41] K.L. White, H.-J. Sue, Electrical conductivity and fracture behavior of epoxy/Polyamide-12/multiwalled carbon nanotube composites, Polym. Eng. Sci. 51 (2011) 2245–2253, https://doi.org/10.1002/pen.21996.

[42] S. Sharma, B.P. Singh, S.S. Chauhan, J. Jyoti, A.Kr. Arya, S.R. Dhakate, V. Kumar, T. Yokozeki, Enhanced thermomechanical and electrical properties of multiwalled carbon nanotube paper reinforced epoxy laminar composites, Compos. Part A Appl. Sci. Manuf. 104 (2018) 129–138, https://doi.org/10.1016/j.compositesa.2017.10.023.

[43] Y. Yang, Z. Pei, X. Zhang, L. Tao, Y. Wei, Y. Ji, Carbon Nanotube–Vitrimer Composite for Facile and Efficient Photo-Welding of Epoxy, Chem. Sci. 5 (2014) 3486–3492, https://doi.org/10.1039/C4SC00543K.

[44] B. Earp, J. Hubbard, A. Tracy, D. Sakoda, C. Luhrs, Electrical behavior of CNT epoxy composites under in-situ simulated space environments, Compos. B Eng. 219 (2021) 108874, https://doi.org/10.1016/j.compositesb.2021.108874.

[45] E. Tzouma, A.S. Paipetis, N.-M. Barkoula, Stress relaxation behavior and electrically activated dynamic exchange in carbon nanotube-modified epoxy Vitrimers, ACS Appl. Polym. Mater. 5 (2023) 172–181, https://doi.org/10.1021/acsapm.2c01412.

[46] K. Tangthana-umrung, X. Zhang, M. Gresil, Synergistic toughening on hybrid epoxy nanocomposites by introducing engineering thermoplastic and carbon-based nanomaterials, Polymer (Guildf.) 245 (2022) 124703, https://doi.org/10.1016/j.polymer.2022.124703.

[47] S.A. Bansal, V. Khanna, Twinkle, A.P. Singh, S. Kumar, Small percentage reinforcement of carbon nanotubes (CNTs) in epoxy(bisphenol-a) for enhanced mechanical performance, Mater. Today Proc. 61 (2022) 275–279, https://doi.org/10.1016/j.matpr.2021.09.225.

[48] J. Xiao, D. Liu, H. Cheng, Y. Jia, S. Zhou, M. Zu, Carbon nanotubes as light absorbers in digital light processing three-dimensional printing of SiCN ceramics from preceramic polysilazane, Ceram. Int. 46 (2020) 19393–19400, https://doi.org/10.1016/j.ceramint.2020.04.282.
[49] G.A. Rance, D.H. Marsh, R.J. Nicholas, A.N. Khlobystov, UV–Vis absorption spectroscopy of carbon nanotubes: relationship between the π-Electron Plasmon and nanotube diameter, Chem. Phys. Lett. 493 (2010) 19–23, https://doi.org/10.1016/j.cplett.2010.05.012.
[50] H. Wang, J. Li, X. Zhang, Z. Ouyang, Q. Li, Z. Su, G. Wei, Synthesis, characterization and drug release application of carbon nanotube-polymer Nanosphere composites, RSC Adv. 3 (2013) 9304, https://doi.org/10.1039/c3ra40997j.
[51] V.G. Pham, N.T. Pham, L.D. Tran, T.H. Dinh, I. Vrublevsky, K. Charniakova, H. V. Le, Insight into the effect of zinc oxide nanoparticles coated multi-walled carbon nanotubes (ZnO/MWCNTs) on the thermal conductivity of epoxy nanocomposite as an electrical-insulating coating, J. Aust. Ceram. Soc. 57 (2021) 1445–1452, https://doi.org/10.1007/s41779-021-00646-6.
[52] B. Alemour, O. Badran, M.R. Hassan, A review of using conductive composite materials in solving lightening strike and ice accumulation problems in aviation, J. Aerosp. Technol. Manag. (2019), https://doi.org/10.5028/jatm.v11.1022.
[53] B.P. Krishnan, K. Saalwaechter, V.K.B. Adjedje, W.H. Binder, Design, synthesis and characterization of Vitrimers with low topology freezing transition temperature, Polymers (Basel) 14 (2022) 2456, https://doi.org/10.3390/polym14122456.
[54] W. Denissen, J.M. Winne, F.E. Du Prez, Vitrimers: permanent organic networks with glass-like fluidity, Chem. Sci. 7 (2016) 30–38, https://doi.org/10.1039/C5SC02223A.
[55] M. Guerre, C. Taplan, J.M. Winne, F.E. Du Prez, Vitrimers: directing chemical reactivity to control material properties, Chem. Sci. 11 (2020) 4855–4870, https://doi.org/10.1039/D0SC01069C.